Desalination and Water Treatment
www.deswater.com
doi: 10.5004/dwt.2020.25722

192 (2020) 33–43
July

Theoretical validation model of a double slope still with forced convection

José Andrés Alanís Navarro[a], Beatriz Castillo-Téllez[b], Rachid Marzoug[b], Margarita Castillo Téllez[c,*]

[a]*Universidad Politécnica del Estado de Guerrero, Taxco de Alarcón, Guerrero, México 40321, email: aalanis@upeg.edu.mx (J.A.A. Navarro)*
[b]*Centro Universitario del Norte, Universidad de Guadalajara, Jalisco, México, emails: beatriz.castillo@academicos.udg.mx (B. Castillo-Téllez), r.marzoug@cunorte.udg.mx (R. Marzoug)*
[c]*Facultad de Ingeniería, Universidad Autónoma de Campeche, Campeche, Campeche, México, email: mcastill@uacam.mx (M.C. Téllez)*

Received 19 June 2019; Accepted 20 February 2020

ABSTRACT

The use of solar energy for water desalination becomes vital for sustainable water supply. This paper aims to analyze the experimental behavior of double slope solar theoretically still (DSSS). In this work, we proposed a theoretical model that can predict the DSSS performance. The theoretical results of temperatures and the impact of wind speed on water production are in good agreement with experimental findings. It is found that the temperature augments with augmenting the wind speed until a critical value, where the temperature starts to drop. In addition, water production increases with increasing speed. In this way, we determined the optimum wind speed to have maximum water production with minimum energy consumption simultaneously. The validation of the theoretical model allows us to predict the DSSS production under different climatic conditions and to scale DSSS dimensions according to the need of water. The salinity of the water is not a determining factor in its production. The production at 4.2 kWh/m^2 daily insolation was 0.58 L/d. The volume of distilled water reaches a maximum value (62.3% efficiency) when glass and environment temperatures are similar. This phenomenon occurs at 5.5 m/s wind speed.

Keywords: Double slope solar still; Theoretical validation; Solar energy; Forced convection; Energy2D

1. Introduction

Given the water shortage situation around the world, a significant number of countries have devoted much effort to obtain fresh water from sources such as the sea, lagoons, or brackish wells. The process of obtaining fresh water from these sources is desalination. Its cost can be very high in terms of energy consumption and environmental quality. The solar still is a straightforward and efficient system that allows reproducing in an accelerated way the natural water cycle. In this context, many studies have been realized to increase the efficiency of this system, especially the double slope solar still (DSSS) type. Rajaseenivasan et al. [1] performed a comparative study on a double slope single basin and double basin solar still; they used various water depths and different materials. It is found that the double basin production is 85% higher than the single basin still. Morad et al. [2] studied the efficiency of a double solar still with a flat-plate solar collector and different cooling glass cover thickness. Wang et al. [3] proposed a design of a novel solar distillation that can use seawater directly in agricultural irrigation.

Also, the use of a double basin attached with vacuum tubes enhances the still performance, based on the results obtained in [4]. Kumar et al. [5] improved the air circulation and vapor condensation, introducing a fan and

* Corresponding author.

external condenser. Somwanshi and Tiwari enhanced the performance of a single basin solar with water flow from an air cooler on the cover [6].

In [7], the authors studied a system that uses solar energy as a pressure source for reverse osmosis (RO) water desalination. Mashaly et al. [8] investigated the performance of a solar desalination system using three different types of feed water to reach near-zero liquid discharge (ZLD) under the hyper-arid environment.

Many researchers aim to develop mathematical models that represent the thermodynamic phenomena to optimize the distillation process, especially to predict the volume of distilled water. Johnson et al. [9] proposed a thermal model for predicting the performance of a solar still with Fresnel lens. They found that the Fresnel lens can help improve the overall efficiency of the solar still. Thermal modeling of a double slope active solar still has been carried out based on the energy balance of east and west glass covers, water mass, and basin liner under natural circulation mode [10]. Kalbasi et al. [11] formulated a mathematical model to predict the performance of single and double effect solar still by using modified heat transfer correlations. Two similar experimental desalination units (single and double effect) were designed to validate the mathematical model. Wind speed is an essential parameter for distillation since it contributes significantly to the condensation process; thus, the increase of efficiency [12].

Recently, a thermal analysis of double slope solar still by using free software called Energy2D is reported [13]. In this work, a theoretical validation of previous experimental studies [2] and analysis of forced convection effects in double slope solar still is performed.

The paper is organized as follows: in section 2, we define used materials and methods. In section 3, the results are discussed, and some findings are reported. Finally, section 4 is dedicated to the conclusions.

2. Experimental study

Two identical double solar stills were designed and manufactured, with a square tray-type solar collector. Their bottom has a side of 0.5 m (0.25 m^2 collection area), constructed using the 16-gauge copper sheet (1.61 mm thick). This bottom was coated with matte black paint resistant to high temperatures to increase solar radiation absorption. The tray was thermally insulated by 0.10 m thickness polyurethane foam to ensure thermal insulation. Finally, this foam was covered with metal to enhance the mechanical structure.

The still's cover is formed by 3 mm thick glass placed at an inclination of 23°. Two aluminum channels with a slight slope and a 0.635 cm perforation, transport, and collect the condensed water. At the center of the DSSS, a container distributes the water to the stills, maintaining a constant level of brackish water to be treated using a 0.635 cm hose. Each still has an independent condensate collector. The brine is eliminated by a hole located at the base of the tray, and the distilled water is continuously recorded (Fig. 1).

To analyze the influence of the wind speed on the evaporation–condensation process of water, a closed wind tunnel constructed of plastic was designed and placed at the roof

Fig. 1. General view of the experimental device.

of one still to control and stabilize the airflow at a different speed. The wind speed is produced inside the tunnel using three fans powered electrically with a variable voltage source. The process of switching on and off is performed automatically during the 8:00–20:00 h period.

The principal objective of this paper is the validation of the experimental results with a theoretical model and simulation that analyzes the influence of wind speed and saline concentration on double slope solar still productivity. In our knowledge, this work has not been treated in the literature.

2.1. Materials and methods

In one still, the air is injected over the glass cover, using a 3 mm thick plate for its speed distribution and control. Air follows the outer contour, forming a tunnel. The effect of placing this double cover was considered in the efficiency still analysis. Three fans (119 mm × 119 mm × 38 mm and a 390 g of weight), with a 0.94 A supply and a variable voltage from 0 to 60 V DC, helped to obtain the desired wind. A digital display shows the voltage and the electrical current consumed by the fans. Fig. 2 shows the detail of the parallel interconnection.

The salted water is supplied during the night to each basin for distillation during the day. The water depth is constant (2 cm). The following variables are collected in real-time: solar radiation, temperatures: ambient, inside of the still, basin water, and wind speed. The distilled water is measured by recording the weight in a precision balance. The measurement cycles are taken at 20:00 h each day. In the beginning, the average wind speed is fixed. To achieve the required speed, three fans of dimensions (119 mm × 119 mm × 38 mm) were used. To measure the mass of distilled water, we used a Tor-Rey electronic scale, L-EQ 5/10 series, with an accuracy of 0.001 kg. A computer records the information every 10 min.

We used two sensors for the recording of wind speed. One integrated into a Skywatch Owners model Geos 11 portable weather station, (±4% accuracy) and a Cole Palmer thermo-anemometer, model EW-10323-11 with a resolution

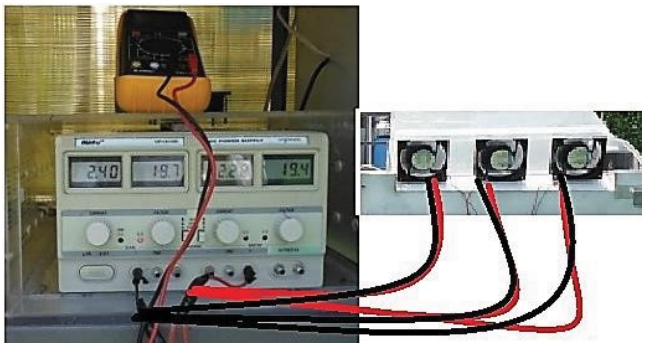

Fig. 2. Detail view of the parallel interconnection of the fans.

of 0.1 m/s. One was used to measure the speed at the surface of the glass cover, and others to measure the speed across the wind tunnel. A picture and schematic diagram of the location of the fans placed in the wind tunnel are shown in Fig. 3.

2.2. Experimental procedure

For the preparation of seawater at the laboratory, we used the salt concentration values reported by Werlinger et al. [14].

The brackish water distribution vessel supplies overnight for daytime operation, keeping the level in each of the constant at 2 cm using the constant level burette. The DSSS is exposed to solar radiation, and the variations in temperatures inside and outside the still, brackish water, the environment, solar radiation, and the selected speed inside the wind tunnel are recorded. The amount of distilled water is measured by recording its weight on the precision balance. The measurement cycles are recorded at 20:00 h of each day. In the beginning, average wind speed is set, and the variations of the different parameters are recorded through an automatic data acquisition system (DAS).

2.3. Instrumentation

The stills were instrumented using *K*-type thermocouples placed inside and outside the device to measure the temperature; using these thermocouples and a DAS Brand Campbell CR10 model, these temperatures were measured daily; installed program extracts data every 10 min through the serial interface that connects to a computer.

Moreover, daily climatological data was acquired: solar irradiance, ambient temperature, wind speed, wind direction, and relative humidity, which are continuously recorded at the Institute of Renewable Energies in Temixco, Morelos, México. Table 1 shows the accuracy and description values given by the manufacturers of the different sensors used in this solarimetric station.

2.4. Experimental and theoretical analysis

The experimental study was carried out at the Institute of Renewable Energies of the National Autonomous University of Mexico, in Temixco, Morelos, México, located at 18°51′NL and 99°14′WL. The experimental device consists of one DSSS with a copper tray coated with black paint (high temperature resistant), 0.25 m^2 of the solar collection area, and 12.5 ± 0.2 L of capacity. The cover is made of standard glass (3 mm thickness) with an inclination of 23° and south-oriented, resulting in an optimal transmittance according to the local latitude. The walls and the bottom were thermally insulated with polyurethane foam (10 mm of thickness), which was covered with a metallic protective shield. The cover and the enclosure was sealed to prevent any vapor and condensate loss. The water depth was 2 cm, which corresponds to a 5.0 L capacity. A second still with the same characteristics with natural convection kept operating at the same time to compare the performance of both. Moreover, the exterior air does not influence the interior wind speed. Fig. 1 shows a general view of the experimental equipment. The purpose of this paper is to validate the experimental results with a theoretical model analyzing the influence of wind speed on DSSS productivity.

2.5. Transient model

The solar irradiance (G) passing through a transparent cover with a transmittance (t) that depends on the material and its thickness ($\tau_g G$). A portion of this radiation is absorbed ($\alpha_g G$) or reflected ($\rho_g G$). The portion of G that reaches the water surface ($\tau_g G$) again undergoes a decomposition due to the optical characteristics of the water; reflected ($\rho_w \tau_g G$), absorbed ($\alpha_w \tau_g G$) and transmitted ($\tau_w \tau_g G$). The most radiation amount transmitted to the base of the tray is absorbed ($\alpha_b \tau_w \tau_g G$), and a small portion is reflected ($\rho_b \tau_w \tau_g G$) because

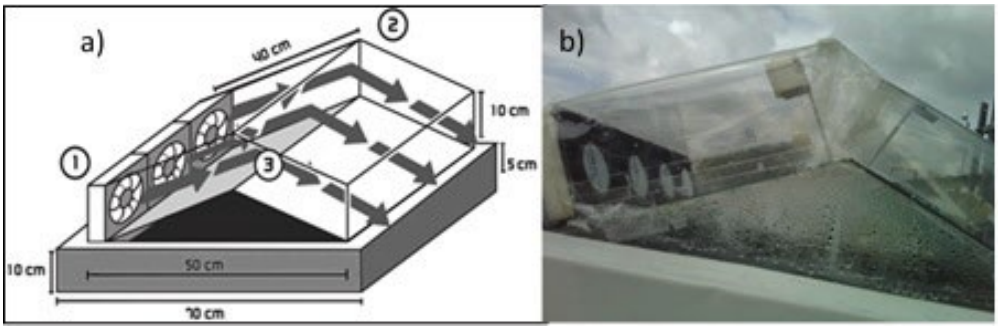

Fig. 3. (a) Schematic diagram and (b) photograph of the location of the fans in the wind tunnel. (1) Fans, (2) glass cover, and (3) wind tunnel.

Table 1
Characteristics and description of the measuring instruments used in this work

Parameter	Description	Model	Calibration	Maximum error
Global irradiation	Pyranometer Eppley	PSP	Annual (IGF-UNAM) (K = 7.68 Sensor Campbell)	±0.5 W/m^2
Ambient temperature and relative humidity	Sensor Campbell, CS500	1,000 ΩPRT, DIN 43760B	Biannual	±0.4°C ±3%
Wind speed and direction	Air Sentry mod 03002-5 R.M. Young Company	03002–5	Biannual	±0.3 m/s ±3°

the black color of the tray base has a high absorptance and low reflectance. The energy absorption in the base of the tray is the necessary energy to heat the water of the tray or absorber. A portion is transmitted to the exterior by conduction through the tray thickness (Q_k). Another part is transferred to the water by convection (Q_{cw}), this heat gained by water, reaches the glass cover from its surface by three heat transfer phenomena: the first part is due to convection through the internal air (Q_c), the second part constitutes the latent heat which transports the vapor molecules that will condense on the inner part of the glass cover (Q_u) which represents precisely the amount of heat necessary to evaporate the water placed in the tray. The third phenomenon is the radiative heat (Q_r) between the water surface and the glass cover. This radiation produces the greenhouse effect. The heat given to the glass is transferred to the exterior due to the convection (Q_{ca}). The overall optical and thermal phenomena that occur in a solar still are illustrated in Fig. 4.

To calculate the still thermal efficiency (η) we used the following equation:

$$\eta = \frac{V \cdot h_{fg}}{P_{av} \cdot H \cdot 3{,}600} \tag{1}$$

where V: distillate volume measured (L); h_{fg}: latent heat of vaporization (J/kg). Its value was obtained considering the maximum temperature obtained in the water to distill;

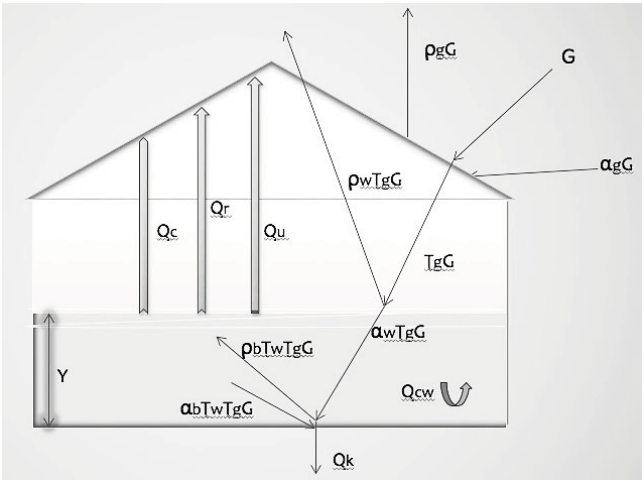

Fig. 4. Phenomena involved in the performance of the solar still.

P: potency of the incidence of solar radiation on the absorber surface (given by the product of the average irradiance I of the day (W/m^2) by the surface S (m^2); H: total exposure time or sun hours (h).

The product $P{\cdot}H{\cdot}3{,}600$ is the solar energy captured by the absorber (J) [15,16]. The energy balance of the still requires that solar radiation absorbed must be equal to the transferred energy from the roof to the air plus the losses of the bottom/walls and the stored energy in the system [17]. The corresponding equations are the following:

Eq. (2) gives the differential equation for the slope:

$$m_g \mathrm{Cp}_g \frac{dT_g}{dt} = \left(\alpha_g I_b + \alpha_g I_d\right) + \left(q_{ev} + q_{r,w-g} + q_{c,g-g}\right) - q_{r,g-\mathrm{air}} + q_{c,g-\mathrm{air}} \tag{2}$$

The heat transferred by evaporation between the water and the cover (q_{ev}) is based on [10]:

$$q_{ev} = 16.28 h_c \left(P_w - P_g\right) \tag{3}$$

And p_w *y* p_g:

$$P_w = e^{(25.317-5{,}144)/T_w} \tag{4}$$

$$P_g = e^{(25.317-5{,}144)/T_w} \tag{5}$$

h_c represents the heat transfer coefficient by convection and is calculated by the following equation:

$$h_c = 0.884\left(T_w - T_g\right) + \left[\frac{\left(P_w - P_g\right)T_w}{\left(268{,}900 - P_w\right)}\right]\left(\mathrm{W/m^2K}\right) \tag{6}$$

The heat transfer from the water to the cover by radiation is given by Stefan–Boltzmann Law, considering that the emittance of the glass cover is 0.9:

$$q_{r,w-g} = 0.9\sigma\left(T_w^4 - T_g^4\right) \tag{7}$$

This heat is due to the radiant exchange between the water surface and the glass cover.

The heat transferred by convection between the absorber and the glass cover consists of the convection of

the air enclosed between the evaporating and condensing surface and is called internal convection. The amount of heat transferred by this phenomenon can be calculated by the following expression, which is modeled by Newton's cooling Law:

$$q_{c,w-g} = h_c\left(T_w - T_g\right) \tag{8}$$

The heat lost by the cover towards the atmosphere by radiation is calculated with the following expression:

$$q_{r,g-\text{air}} = 0.9\sigma\left(T_g^4 - T_{\text{sky}}^4\right) \tag{9}$$

The exterior temperature depends on the amount of water vapor and dust in the atmosphere, which will be manifested in an increase in the heat reflectance of the soil. The used Eq. (10) to find this value is [18]:

$$T_{\text{sky}} = T_{\text{air}}\left[0.74 + \left(0.006T_{\text{dp}}\right)\right]^{0.25} \tag{10}$$

where T_{dp} is the dew point temperature of the ambient air and can be calculated by [19]:

$$T_{\text{dp}} = \frac{237.3K\left(\ln\varnothing + \dfrac{17.27T_{\text{amb}}}{T_{\text{amb}} + 237.3K}\right)}{17.27 - \left(\ln\varnothing + \dfrac{17.27T_{\text{amb}}}{T_{\text{amb}} + 237.3K}\right)} \tag{11}$$

The heat transfer by convection between the glass cover and the ambient air is given by:

$$q_{c,g-\text{air}} = h_g\left(T_g - T_{\text{air}}\right) \tag{12}$$

The following Eq. (13) calculates the coefficient of heat transfer by convection between the booth and the air:

$$h_g = \left(\text{Nu}_L + \text{Nu}_f\right)^{1/3} k_g / L_g \tag{13}$$

The energy balance Eq. (14) for the absorber is calculated by:

$$m_b\text{Cp}_b\frac{dT_b}{dt} = q_{r,b} - q_{c,w-b} - \left(q_k + q_x\right) \tag{14}$$

The heat transfer coefficient for the equation that models this convection is calculated according to the following equation:

$$q_{c,w-b} = h_b\left(T_w - T_b\right) \tag{15}$$

The heat transfer coefficient between the water and the absorber ($q_{c,w-b}$), is calculated using the following Eq. (16) [20]:

$$h_b = \text{Nu}\frac{k_w}{L_b} \tag{16}$$

The last term in the Eq. (17) represents the heat losses by conduction of the base and sides of the absorber into ambient air and is modeled by Fourier's law:

$$\left(q_k + q_x\right) = \frac{k_b\left(T_b - T_{\text{amb}}\right)}{L_b} \tag{17}$$

The energy balance Eq. (18) for the insulation of the absorber is:

$$m_{\text{in}}\text{Cp}_{\text{in}}\frac{dT_{\text{in}}}{dt} = \left(q_k + q_x\right) - q_{\text{loss}} \tag{18}$$

The heat loss by the insulator can be written:

$$q_{\text{loss}} = U_{\text{in}}\left(T_{\text{in}} - T_{\text{air}}\right) \tag{19}$$

The total heat transfer coefficient of the insulator U_{in} is calculated by:

$$U_{\text{in}} = \left(\frac{L_{\text{in}}}{k_{\text{in}}} + \frac{1}{h_{\text{in}}}\right)^{-1} \tag{20}$$

In the same way as in the previous two Eqs. (19) and (20), the convection coefficient (h_{in}) is calculated by the Dunkle [15]:

$$h_{\text{in}} = \text{Nu}_{\text{in}}\frac{k_{\text{air}}}{L_{\text{in}}} \tag{21}$$

The energy balance Eq. (22) of water is calculated by:

$$m_w\text{Cp}_w\frac{dT_w}{dt} = \frac{\left[\left(\alpha_w\tau_g I + q_{c,w-b}\right) - \left(q_{r,w-g} + q_{c,w-g} + q_{\text{ev}}\right)\right]}{\rho_w\text{Cp}_w L_w} \tag{22}$$

k_w is the water thermal conductivity and L_b is the characteristic length of the copper plate, evaluating both the base and the height of the basin.

2.5.1. Numerical solution and computational model

The theoretical study presented is based on the experimental results carried out in a DSSS. An acrylic sheet 3 mm thickness was adapted on the glass cover with an optical transmission in the visible interval of 80.7% to create a "wind tunnel" and the greenhouse effect. Three fans were placed symmetrically to ensure a uniform air flux throughout the inner surface of the roof (forced convection). This airstream over the hot sheet enhances the heat convection phenomenon. The parameters that affect the equations of gain and loss of the energy in the solar still depends on the climatic conditions during the day, Fig. 5. To evaluate these equations, different heat values that depend on the temperatures must be determined. The modeling process begins with a proposed value for each temperature of the glass cover $T_{g,t}$, absorber $T_{b,t}$ insulator $T_{\text{in},t}$ and water $T_{w,t}$. The ambient temperature is considered as a starting point for

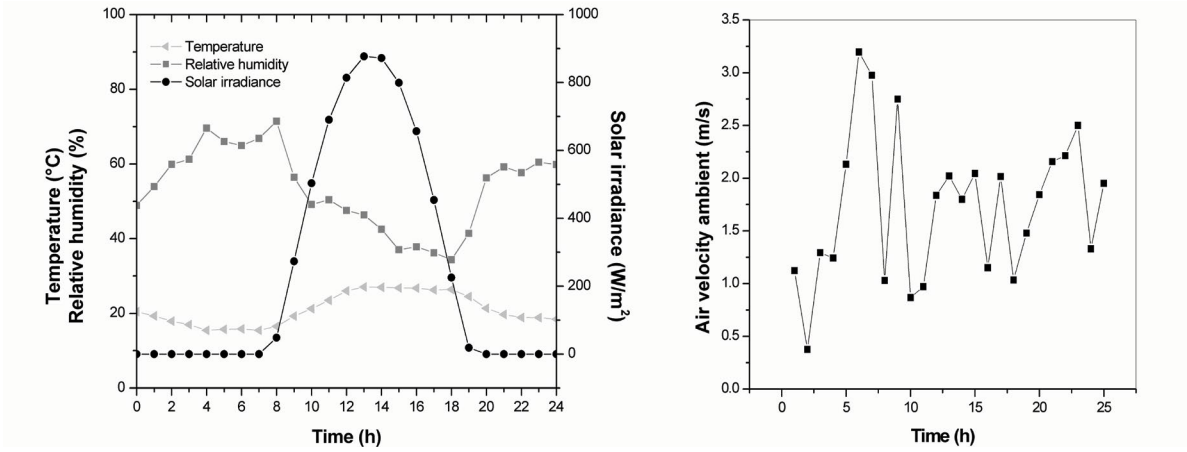

Fig. 5. Climatological parameters affecting distillation.

all equations. To solve these equations, we used the finite difference method [21]. Eqs. (6)–(9) were discretized and Access software was used as a computational tool to implement the solution. The simulation was performed using 1 h between two successive iterations Δt = 1 h.

$$T_{g,t+\Delta t} = \frac{\Delta t\left[\begin{array}{l} S\left(\left(\alpha_g \alpha_g G\right)_t + \left(q_{\mathrm{ev},t} + q_{r,w-g,t} + q_{c,w-g,t}\right)\right) \\ -q_{r,g-\mathrm{amb},t} - q_{c,g-\mathrm{amb},t} \end{array}\right]}{m_g \mathrm{Cp}_g} + T_{g,t} \quad (23)$$

$$T_{b,t+\Delta t} = \frac{\Delta t\left[\left(q_{b,t} + q_{c,w-b,t}\right) - \left(q_k + q_{x'}\right)_t\right]}{m_b \mathrm{Cp}_b} + T_{b,t} \quad (24)$$

$$T_{\mathrm{in},t+\Delta t} = \frac{\Delta t\left[\left(q_k + q_{x'}\right)_t - q_{\mathrm{loss}_t}\right]}{m_{\mathrm{in}} c_{\mathrm{in}}} + T_{\mathrm{in},t} \quad (25)$$

$$T_{w,t+\Delta t} = \frac{\Delta t\left[S\left(\left(\alpha_w \tau_g I_d\right)_t + q_{c,w-b,t}\right) - \left(q_{r,w-g,t} + q_{c,w-g,t} + q_{\mathrm{ev},t}\right)\right]}{\rho_w \mathrm{Cp}_w L_w} \quad (26)$$

To calculate the instantaneous distilled water for time t, we used the following equation:

$$\mathrm{Pro} = \frac{Q_{\mathrm{ev}}}{h_{\mathrm{fg}}} \quad (27)$$

A table with real-time temperature values of the cover, absorber, insulator, and water, is also introduced into the program. These initial temperatures are used to solve the equations of each heat transfer type (radiation, convection, and evaporation). The obtained heats are utilized in each new discretized equation.

2.5.2. Physical model

The experimental results it was complemented by performed simulations using the computational fluid dynamics technique, with a general-purpose commercial computing program Fluent from the company ANSYS (Headquartered in the United States, South of Pittsburgh in Canonsburg, Pennsylvania) [22]. This software includes design tools in three dimensions (3D), the solution of the mathematical equations that represent the phenomena studied, such as heat transfer, etc., is obtained by the finite volume method (FVM), through a process of discretization finding approximate solutions of partial differential equations [23]. The simulation consists of four stages: (i) design and definition of properties of the materials, (ii) mesh or sub-division of the 3D space, (iii) solution of the equations by the FVM [24], and (iv) presentation of results and analysis (flow chart of Fig. 6 [25]). This simulation is useful to know the speed and temperature fields inside solar water still. The design was made according to the physical dimensions and materials of the manufactured still. For the mesh of the still, 405,970 volumes of the tetrahedron type was used (Fig. 7). The elements quality of the mesh was evaluated using the parameter of "angle bias" and the equiangular and equi-size skew. These two parameters are less than 0.5 for 92% and less than 0.25 for 51% of the elements; a value = 1 means a high bias of the elements, which causes erroneous results.

3. Results and discussions

In order to analyze the production of distilled water, experiments with two solar stills working with seawater and drinking water, natural convection, and functioning simultaneously. Fig. 8 shows the water production obtained in each still. It can be seen that regardless of the solar energy received, daily production decreases as the salt concentration increases. However, salt concentration has no significant influence on the final amount of distilled water. Therefore, with a solar resource of 4.2 kWh/m^2, the average water production is 0.58 and 0.56 L, while for a solar resource of 3.6 kWh/m^2, 0.49 and 0.47 L are obtained with fresh seawater, respectively. These values are in good agreement with the literature [26,27].

For the brackish water case, initial concentration was 24 ± 0.1 g/L, and remaining not distilled water has a 27.4 ± 0.1 g/L concentration. These results are consistent with those obtained by [28,29].

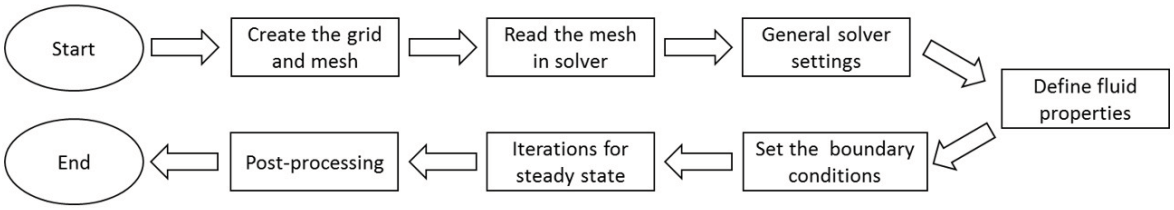

Fig. 6. Flow chart of the finite volume method. Adapted from [20].

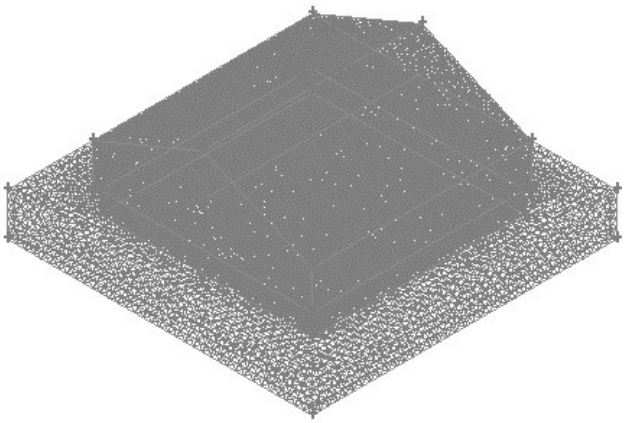

Fig. 7. Isometric view of the still's design with the mesh.

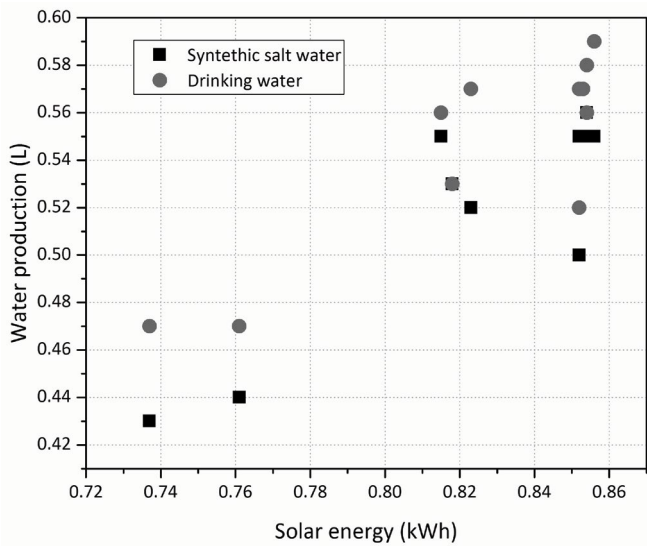

Fig. 8. Water production based on the solar energy received in the collector.

The use of a conductivity meter Thermo Scientific Orion Star A212 brand provided information to determine the salinity of seawater (range from 0.001 to 3,000 μS, 0.001 μS, and accuracy of 0.5%).

Fig. 9 shows a comparison between the irradiance and temperatures measured in the black tray at the different air velocities analyzed. It can be seen that at 6.9 m/s speed, ambient temperature is higher than the outside glass because the glass cools, inferring that under these conditions, there will be less condensation and, consequently, a decrease in water production.

3.1. Comparison of the theoretical model with the experimental data

Fig. 10 shows experimental and theoretical temperatures as a function of time. For all temperatures (T_b, T_g, T_w, and T_{in}), simulation and experimental results are similar. When the irradiance is lower, all these temperatures are almost the same. However, at midday (high irradiance) where the temperature reaches its maximum, the difference between them is significant.

Fig. 11 presents a comparison between the measured irradiance and water production. In this case, the temperature rises and enhances the evaporation, which augments the still efficiency. Also, is presented the experimental results of distilled water and the estimated production by the theoretical model on the same day at 3.5 m/s wind speed. The maximum water yield is obtained approximately at 13:00 h in both cases. Moreover, the theoretical and experimental curves have almost the same qualitative and quantitative behavior. The average deviation was ±0.052 L/h. The impact of the wind speed on the production of distilled water is directly related to the temperature difference between the glass and the water to be distilled. It increases with the decrease in the temperature of the roof. The heat transfer by convection from the deck to the ambient air increases when the heat transfer by evaporation and convection between the water and the house increases. These results are consistent with those reported in [30].

Table 2 shows data obtained in the still with different wind speeds. During test days, the average maximum irradiance (800 W/m^2) was presented at noon, corresponding to 5.53 kWh/m^2 daily, and the amount of distilled water obtained was 0.7 L.

3.2. Simulation

For the simulation of the solar stills behavior, it is necessary to consider the properties of the used materials in the experiments, such as mass density, specific heat, thermal conductivity, among others, not to underestimate or overestimate the obtained results. It is necessary to reach the number of iterations until the solution of the equations converges to a fixed value, usually is 0.001 for the continuity and momentum conservation equations and 1×10^{-6} for the energy equations. Once this value is reached, it is possible

to find the variables information. The distribution of the wind speed vectors inside the double slope is presented at the left of Fig. 12. The bottom temperature of the wind tunnel is higher, which decreases the air density in this region; thus, the wind speed augments. The increasing of the forced convection decreases the solar still temperature, as shown at the right of Fig. 12. Hence, this effect accelerates heat transfer from the absorber to the top, and then the water temperature is reduced.

The effect of wind speed on the temperature distribution on the surface of the absorber was also analyzed. The initial temperature of the absorber is 80°C. It is evident that the temperature on the surface of the absorber decreases with higher speed; these results are shown in Fig. 13. However, the area that is interesting to cool, that is, the glass cover, would allow a higher rate of water vapor condensation, and this should be reflected directly in an increase in the efficiency of water distillation.

Nevertheless, another satisfying result of this investigation shows the dependence of water production on wind speed, as shown in Fig. 14. For low wind speed $v \leq 5.5$ m/s, the water production increases with increasing wind speed. After this critical speed, water production does not exhibit a linear relationship with wind speed. In this case, water production shrinks with the augmentation of wind speed. Furthermore, we can have maximum production with two speeds; 5.5 and 3.5 m/s. Nevertheless, this last wind speed is the optimum one because we can have maximum water production with a minimum energy consumption. This theoretical result is in good agreement with experimental findings in [12].

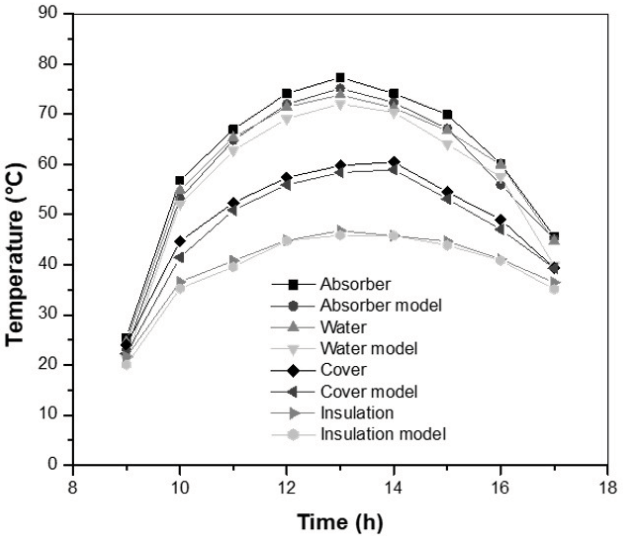

Fig. 10. Theoretical and experimental temperatures during the day.

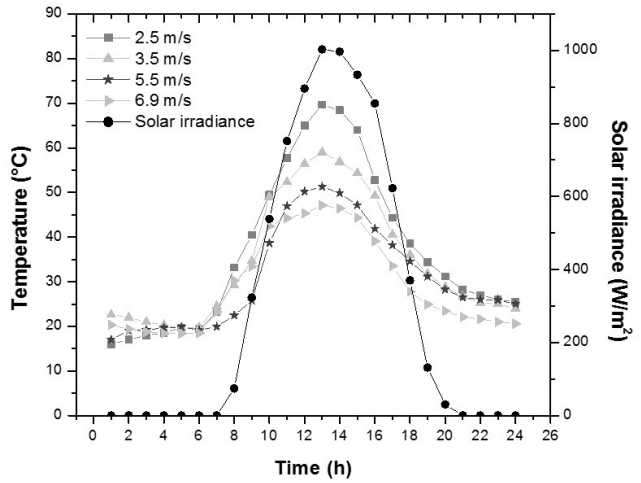

Fig. 9. Comparison between the irradiance and temperatures in the black tray at 2.5, 3.5, 5.5, and 6.9 m/s.

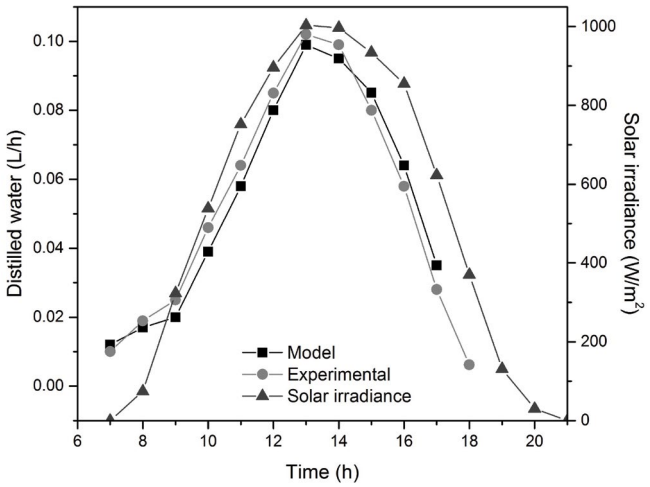

Fig. 11. Experimental and theoretical water production during the day.

Table 2
Comparison of the production of distilled water at different wind speed concerning the solar radiation received.

Average speed (m/s)	Average irradiation (kWh/m²)	Solar energy received in the collector (kWh)	Distilled water* obtained (L/d)	*h* (%)
2.5	5.22	0.860	0.61	46.4
3.5	5.18	0.854	0.75	58.0
5.5	4.91	0.810	0.76	62.3
6.9	5.10	0.842	0.62	48.9

*Manufacturer specified error (scales Tor-Rey): ±0.05 kg

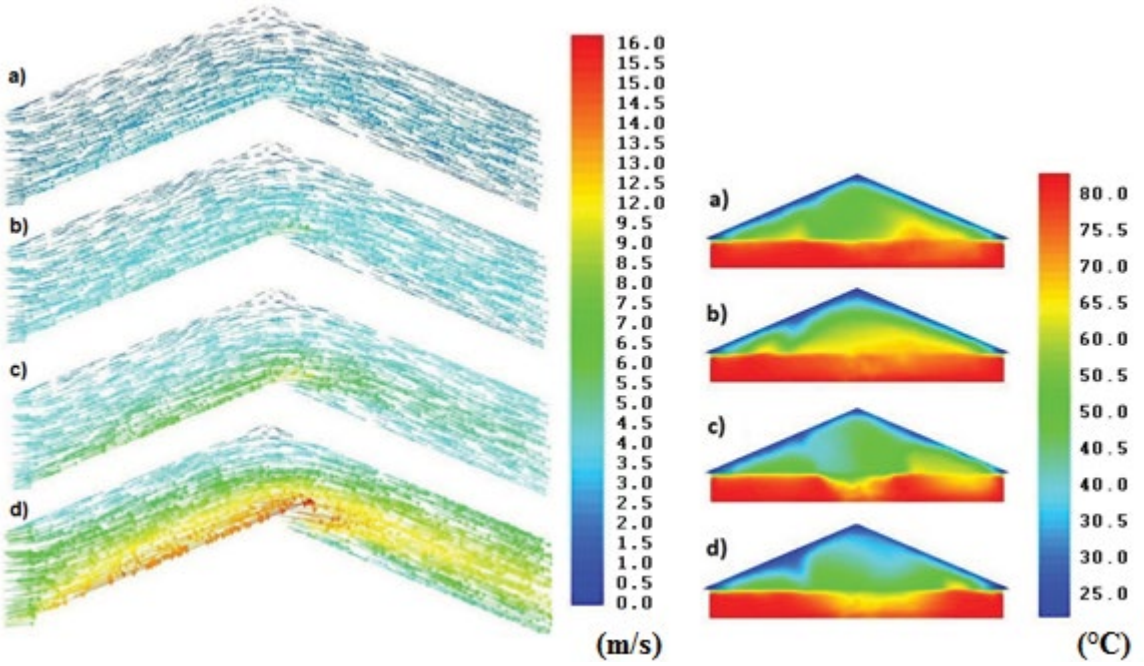

Fig. 12. Vectors speed in the double slope (left). Temperature profiles inside the house and the absorber at different speed (right): (a) 2.5 m/s, (b) 3.5 m/s, (c) 5.5 m/s, and (d) 6.9 m/s.

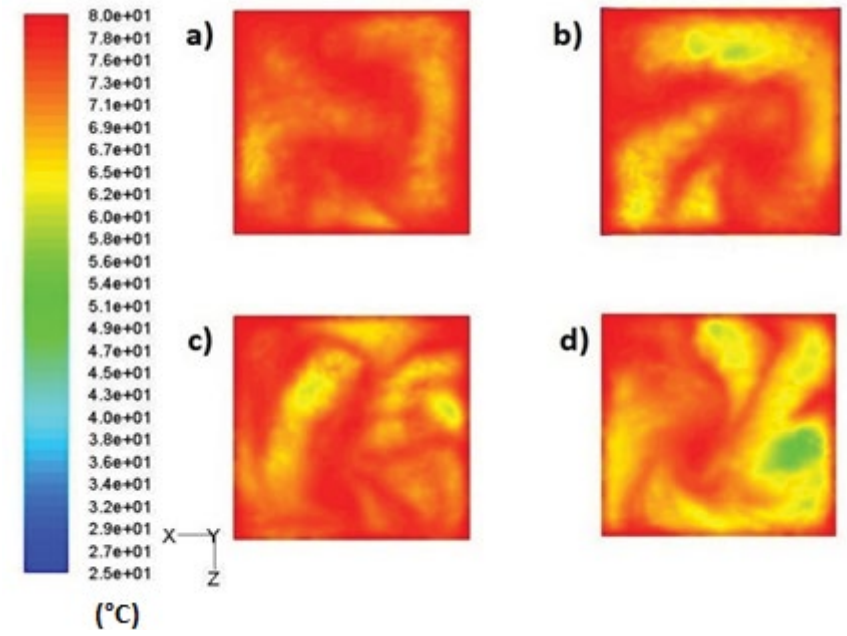

Fig. 13. Temperature distribution at the base of the absorber for different wind speed: (a) 2.5 m/s, (b) 3.5 m/s, (c) 5.5 m/s, and (d) 6.9 m/s.

4. Conclusions

The thermal behavior of two stills built working with natural convection was analyzed. It is found that under the conditions in which the experiment was conducted, the water production is not affected by the salinity. With a typical solar resource of 4.2 kWh/m^2, the analyzed house still is capable to produce 0.58 L/d in the winter. By increasing the wind speed from 0 to 6.9 m/s, the volume of distilled water is increased to a maximum value that is reached when the glass cover has the same temperature as the environment. This result is achieved when wind speed is 5.5 m/s. Moreover, the volume of water obtained was 0.76 L at 4.9 kWh/m^2. The efficiency obtained for these values is 62.3%, which is higher than the researcher

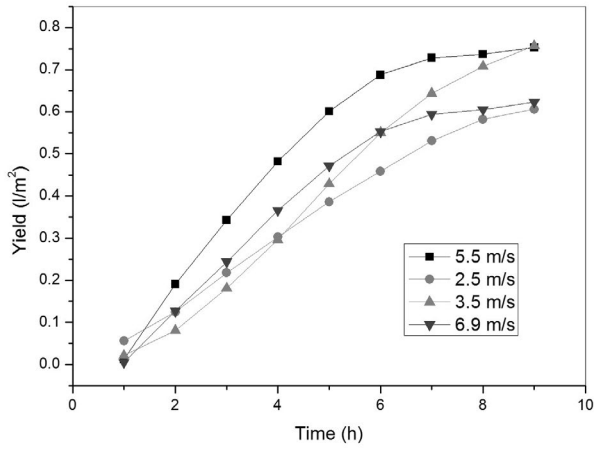

Fig. 14. Water production as a function of time and wind speed.

Cooper estimate for single-house distillers without the influence of roof cooling. For higher speed, the glass temperature was lower than that of the environment, which decreases the volume of distilled water.

Acknowledgments

The authors are grateful for the academic and financial support to develop this research to the Universidad Politécnica del Estado de Guerrero, and M.C. Guadalupe Manuel Estrada Segovia, Director of the Facultad de Ingeniería of the Universidad Autónoma de Campeche.

Symbol

α	—	Absorbance, 1
η	—	Efficiency, 1
ρ	—	Mass density, kg/m^3
τ	—	Transmittance, 1
c_p	—	Specific heat, J/kg/K
h	—	Convective heat transfer coefficient, W/m^2/K
h_{fg}	—	Latent heat of vaporization, J/kg
H	—	Total exposure time, h
I, G	—	Solar irradiance, W/m^2
k	—	Thermal conductivity, W/m/K
L	—	Length, thickness, depth, m
m	—	Mass, kg
Nu	—	Nusselt number, 1
P	—	Solar power, W
Pro	—	Production of distilled water, L
q	—	Heat rate transfer, W
Q	—	Energy transfer, J
S	—	Surface of tray, m^2
t	—	Time, S
T	—	Temperature, K
U	—	Total heat transfer coefficient, m^2/K/W
V	—	Distillate volume, L

Subscripts

a, air	—	Air
amb	—	Ambient
b	—	Basin or tray
c	—	Convective
d	—	Diffuse
dp	—	Dew point
ev	—	Evaporative
g	—	Glass
in	—	Insulator
k	—	Vertical tray thickness
loss	—	Losses
r	—	Radiative
u	—	Upper
w	—	Water
x	—	Horizontal tray thickness

References

[1] T. Rajaseenivasan, T. Elango, K. Kalidasa Murugavel, Comparative study of double basin and single basin solar stills, Desalination, 309 (2013) 27–31.
[2] M.M. Morad, H.A.M. El-Maghawry, K.I. Wasfy, Improving the double slope solar still performance by using flat-plate solar collector and cooling glass cover, Desalination, 373 (2015) 1–9.
[3] Q. Wang, S. Liang, Z. Zhu, G. Wu, Y. Su, H. Zheng, Performance of seawater-filling type planting system based on solar distillation process: numerical and experimental investigation, Appl. Energy, 250 (2019) 1225–1234.
[4] H.N. Panchal, Enhancement of distillate output of double basin solar still with vacuum tubes, J. King Saud Univ. Eng. Sci., 27 (2015) 170–175.
[5] R.A. Kumar, G. Esakkimuthu, K.K. Murugavel, Performance enhancement of a single basin single slope solar still using agitation effect and external condenser, Desalination, 399 (2016) 198–202.
[6] A. Somwanshi, A.K. Tiwari, "Performance enhancement of a single basin solar still with flow of water from an air cooler on the cover", Desalination, 352 (2014) 92–102.
[7] A.A.A. Attia, Thermal analysis for system uses solar energy as a pressure source for reverse osmosis (RO) water desalination, Sol. Energy, 86 (2012) 2486–2493.
[8] A.F. Mashaly, A.A. Alazba, A.M. Al-Awaadh, Assessing the performance of solar desalination system to approach near-ZLD under hyper-arid environment, Desal. Water Treat., 57 (2016) 12019–12036.
[9] A. Johnson, L. Mu, Y.H. Park, D.J. Valles-Rosales, H. Wang, P. Xu, K. Kota, S. Kuravi, A thermal model for predicting the performance of a solar still with fresnel lens, Water, 11 (2019) 1860.
[10] V.K. Dwivedi, G.N. Tiwari, Experimental validation of thermal model of a double slope active solar still under natural circulation mode, Desalination, 250 (2010) 49–55.
[11] R. Kalbasi, A.A. Alemrajabi, M. Afrand, Thermal modeling, and analysis of single and double effect solar stills: an experimental validation, Appl. Therm. Eng., 129 (2018) 1455–1465.
[12] M. Castillo-Téllez, I. Pilatowsky-Figueroa, Á. Sánchez-Juárez, J.L. Fernández-Zayas, Experimental study on the air velocity effect on the efficiency and freshwater production in a forced convective double slope solar still, Appl. Therm. Eng., 75 (2015) 1192–1200.
[13] J.A. Alanís Navarro, M. CastilloTéllez, M.A. Rivera Martínez, G. Pedroza Silvar, F.C. Martínez Tejeda, Computational thermal analysis of a double slope solar still using Energy2D, Desal. Water Treat., 151 (2019) 26–33.
[14] Werlinger, Camilo, Krisler Alveal, Héctor Romo, Biología marina y oceanografía: conceptos y procesos. Consejo Nacional del Libro y la Lectura, 2004.
[15] R.V. Dunkle, Solar Water Distillation: The Roof Type Still and a Multiple Effect Diffusion Still, In Proc. International Heat Transfer Conference, University of Colorado, USA, 1961, vol. 5, pp. 895.

[16] M.A.S. Malik, V.V. Tran, A simplified mathematical model for predicting the nocturnal output of a solar still, Sol. Energy, 14 (1973) 371–385.
[17] H. Al-Hinai, M.S. Al-Nassri, B.A. Jubran, Effect of climatic, design and operational parameters on the yield of a simple solar still, Energy Convers. Manage., 43 (2002) 1639–1650.
[18] M.N. Bahadori, Passive and Hybrid Convective Cooling Systems, International Passive and Hybrid Cooling Conference, American Section of the International Solar Energy Society, Miami Beach, Florida, Nov. 1981, pp. 715–727.
[19] C. Beck, K. Crowther, H. Kessler, Radiative Cooling: Resource and Applications, Los Angeles, CA, 1981.
[20] J.R. Welty, C.E. Wicks, R.E. Wilson, G.L. Rorrer, Fundamentals of Momentum, Heat, and Mass Transfer, 5th ed., Hamilton Printing, United States of America, 2008.
[21] I.N. Bronshtein, K.A. Semendyayev, G. Musiol, H. Muehlig, Handbook of Mathematics, 5th ed., Springer-Verlag, New York, 2015.
[22] ANSYS, Engineering Simulation & 3D Design Software | ANSYS, 2019. Available at: https://www.ansys.com/ [Accessed: 03-Jun-2019].
[23] E. Oñate, S. Idelsohn, O.C. Zienkiewicz, R.L. Taylor, A finite point method in computational mechanics. Applications to convective transport and fluid flow, Int. J. Numer. Methods Eng., 39 (1996) 3839–3866.
[24] F. Moukalled, L. Mangani, M. Darwish, The Finite Volume Method in Computational Fluid Dynamics, Vol. 113. Berlin, Germany, Springer, 2016.
[25] M. Ahsan, Numerical analysis of friction factor for a fully developed turbulent flow using k–ε turbulence model with enhanced wall treatment, Beni-Suef Univ. J. Basic Appl. Sci., 3 (2014) 269–277.
[26] J.J. Hermosillo, D. Gudiño, Notas Sobre el Curso de Energía Solar, Tlaquepaque, Jalisco, ITESO, 1995, pp. 158.
[27] S.H. Soliman, Effect of wind on solar distillation, Sol. Energy, 13 (1972) 403–415.
[28] R. Kalbasi, M.N. Esfahani, Multi-effect passive desalination system, an experimental approach, World Appl. Sci. J., 10 (2010) 1264–1271.
[29] M.N.I. Sarkar, A.I. Sifat, S.M.S. Reza, M.S. Sadique, A review of optimum parameter values of a passive solar still and a design for southern Bangladesh, Renewables: Wind, Water, Solar, 4 (2017) 1–13.
[30] A.F. Muftah, M.A. Alghoul, A. Fudholi, M.M. Abdul-Majeed, K. Sopian, Factors affecting basin type solar still productivity: a detailed review, Renewable Sustainable Energy Rev., 32 (2014) 430–447.